Modeling and damping of high-frequency leakage currents in PWM inverter-fed AC motor drive systems

Satoshi Ogasawara
Okayama University

Hirofumi Akagi
Okayama University

Modeling and Damping of High-Frequency Leakage Currents in PWM Inverter-Fed AC Motor Drive Systems

Satoshi Ogasawara, *Member, IEEE,* and Hirofumi Akagi, *Fellow, IEEE*

Abstract— **This paper presents an equivalent circuit for high-frequency leakage currents in pulsewidth modulation (PWM) inverter-fed ac motors, which forms a series resonant circuit. The analysis based on the equivalent circuit leads to such a conclusion that the connection of a conventional common-mode choke or reactor in series between the ac terminals of a PWM inverter and those of an ac motor is not effective to reduce the rms and average values of the leakage current, but effective to reduce the peak value.**

Furthermore, this paper proposes a common-mode transformer which is different in damping principle from the conventional common-mode choke. It is shown theoretically and experimentally that the common-mode transformer is able to reduce the rms value of the leakage current to 25%, where the core used in the common-mode transformer is smaller than that of the conventional common-mode choke.

I. Introduction

An increase in the carrier frequency of pulsewidth modulation (PWM) inverters results in a nonnegligible amount of high-frequency leakage current which may cause a serious problem. It would flow through stray capacitors between stator windings and a motor frame due to a large step change of the common-mode voltage produced by a PWM inverter. The peak value may reach the rated current in the worst case. It may have an undesirable influence on the motor current control and may result in incorrect operation of residual current-operated circuit breakers. Furthermore, the leakage current may cause electromagnetic interference (EMI) to electronic equipment, e.g., AM radio receivers, because its oscillation has a frequency in a range from 100 kHz to several MHz [1], [2]. However, few papers on the leakage current have been reported.

This paper proposes an equivalent circuit for the leakage current, which forms a series resonant circuit. The validity of the equivalent circuit and the physical property of each component in the equivalent circuit are confirmed experimentally in detail. As a result, a motor model, including the stray capacitors, is also proposed, which is applicable to the analysis of both normal-mode and common-mode currents.

Paper IPCSD 96–20, approved by the Industrial Drives Committee of the IEEE Industry Applications Society for presentation at the 1995 IEEE Industry Applications Society Annual Meeting, Lake Buena Vista, FL, October 8–12. Manuscript released for publication March 19, 1996.

The authors are with Okayama University, Okayama, 700 Japan.

Publisher Item Identifier S 0093-9994(96)05777-5.

A common-mode choke has been used to reduce the undesirable leakage current, which is connected in series between the terminals of an inverter and those of a motor [3]–[5]. Analysis on the basis of the proposed equivalent circuit results in the following conclusion: The connection of the conventional common-mode choke is not effective to reduce the rms and average values of the leakage current, but effective to reduce the peak value. The analytical result is also verified by experiment.

Furthermore, this paper proposes a common-mode transformer capable of reducing the leakage current. The common-mode transformer is characterized by such a simple configuration that another isolated winding, the terminals of which are shorted by a damping resistor, is added to the common-mode choke. Thus, the authors named it the "common-mode transformer" which corresponds to the term of the conventional "common-mode choke." The common-mode transformer does not play any role for the normal-mode voltage and current, while it acts as the damping resistor for the common-mode voltage and current. Therefore, it can damp the oscillation of the leakage current, dissipating a negligible amount of loss in the resistor. This damping principle is different from the conventional common-mode choke, and already proposed suppression circuits [5], [6]. The suppression circuits consist of four tightly coupled coils equipped with RC circuits. It is shown that a common-mode transformer, the core size of which is smaller than that of a conventional common-mode choke, is able to reduce the rms value of the leakage current to 25%. A design procedure of the common-mode transformer is also discussed in detail.

II. High-Frequency Leakage Currents

A. Common-Mode Voltage

Fig. 1 shows a voltage-source inverter connected to a motor which is represented by three inductors and resistors. A set of voltage-current equations is given by

$$\left.\begin{aligned} v_a - v_n &= R_m i_a + L_m \frac{di_a}{dt} \\ v_b - v_n &= R_m i_b + L_m \frac{di_b}{dt} \\ v_c - v_n &= R_m i_c + L_m \frac{di_c}{dt} \end{aligned}\right\} \quad (1)$$

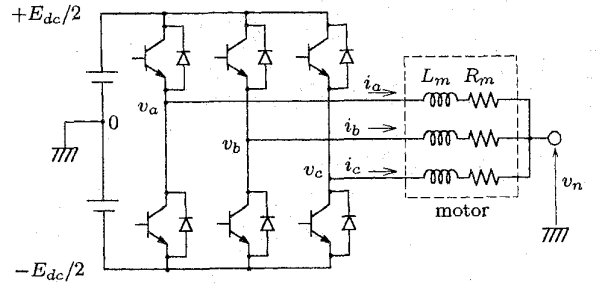

Fig. 1. Three-phase voltage-source inverter.

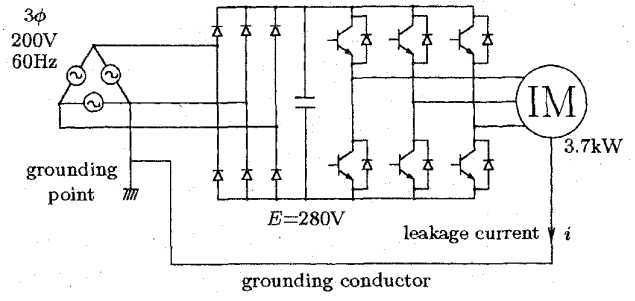

Fig. 2. Experimental system.

TABLE I
RATINGS OF TESTED INVERTER AND INDUCTION MOTOR

input voltage	3φ 200	V
rated current	21.0	A
maximum current	52.0	A
modulation scheme	sinusoidal PWM	
carrier frequency	2.4	kHz
rated output	3.7	kW
rated torque	23.5	Nm
maximum torque	70.6	Nm
motor speed	1500/2000	r/min

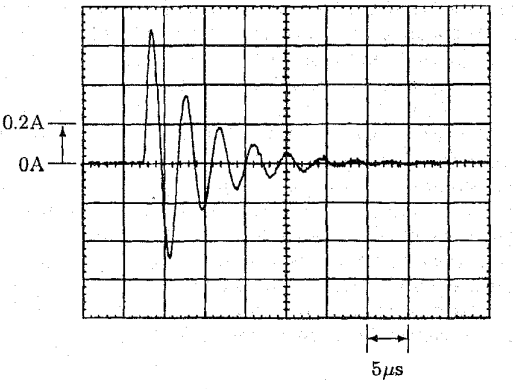

Fig. 3. Leakage current waveform.

where

v_a, v_b, v_c inverter phase voltages;
i_a, i_b, i_c motor line currents;
v_n neutral voltage.

The neutral voltage of the motor corresponds to the common-mode voltage in Fig. 1. Adding the set of equations derives the following equation:

$$v_a + v_b + v_c - 3v_n = \left(R_m + L_m \frac{d}{dt}\right) \cdot (i_a + i_b + i_c). \quad (2)$$

Since $i_a + i_b + i_c = 0$, the common-mode voltage in the motor is calculated by

$$v_n = \frac{v_a + v_b + v_c}{3}. \quad (3)$$

It is shown that only the switching state decides the common-mode voltage regardless of the motor impedance. The common-mode voltage changes by $E_{dc}/3$ every switching of the inverter. The common-mode voltage produced by the inverter forces the leakage current, which is discussed in this paper, to flow through stray capacitors between the motor windings and the motor frame.

B. Modeling for High-Frequency Leakage Currents

Fig. 2 shows an experimental system to measure the leakage current. An induction motor is driven by a voltage-source PWM inverter, and the motor frame is grounded for safety. The leakage current flows from the motor frame through the grounding conductor. Table I shows the ratings of the tested inverter and induction motor.

Fig. 3 shows a leakage current waveform when a phase in the PWM inverter is switched. In this case, the switching gives a step-wise change to the common-mode voltage in the induction motor by 1/3 of the dc link voltage, that is, 280/3 V. It is shown that a nonnegligible amount of oscillatory leakage current flows through the stray capacitors between the stator windings and the motor frame.

A virtual grounding point[1] is introduced to avoid the influence of an internal impedance between the earth terminal on the switch board and the actual grounding point. Three capacitors, the capacitance of which is much larger than the stray capacitance of the motor, are connected to the three-phase input terminals of the rectifier. The grounding conductor is connected to the neutral point of the capacitors, which is considered a virtual grounding point. In the experimental system, the three capacitors of 3 μF are used for providing the virtual grounding point. Comparing the leakage current waveform with that in case of connecting the grounding conductor to the earth terminal, has confirmed that the two waveforms are almost the same. The internal inductance upstream of the earth terminal has been estimated as 10 μH by the experiment.

The authors propose an equivalent circuit for the leakage current, which forms an LCR series resonant circuit shown in Fig. 4, because Fig. 3 is similar to the waveform of current after a step voltage is applied to the resonant circuit. If a step-wise voltage is applied to the LCR series resonant circuit, the

[1]The configuration is shown in Fig. 12.

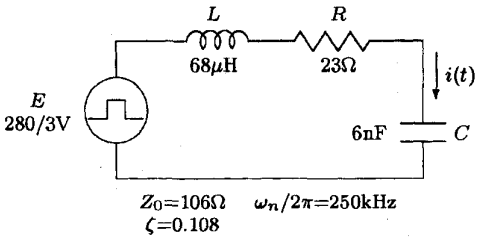

Fig. 4. Equivalent series resonant circuit.

damped and oscillatory current is given as follows:

$$i(t) = \frac{E}{\sqrt{1-\zeta^2}\,Z_0} e^{-\zeta\omega_n t} \sin \sqrt{1-\zeta^2}\,\omega_n t \qquad (4)$$

where

$$\omega_n = \frac{1}{\sqrt{LC}}$$
$$\zeta = \frac{R}{2}\sqrt{\frac{C}{L}}$$
$$Z_0 = \sqrt{\frac{L}{C}}$$

and ω_n, ζ, and Z_0 mean the natural frequency, i.e., the resonant frequency, the damping factor, and the characteristic impedance, respectively. In the case of $1 \gg \zeta^2$, the current flowing in the resonant circuit is approximated to the following equation:

$$i(t) \simeq \frac{E}{Z_0} e^{-\zeta\omega_n t} \sin \omega_n t. \qquad (5)$$

Therefore, the characteristic impedance Z_0 determines the peak value of the oscillatory current. The circuit constants described in the equivalent circuit in Fig. 4 have been estimated from the experimental waveform.

C. Discussion on Equivalent Circuit Constants

The validity of the equivalent circuit and the physical property of each component in the equivalent circuit will be discussed.

In order to take stray capacitors existing in the motor into consideration, two motor models shown in Fig. 5 are compared. In case of Fig. 5(a), the leakage current flowing through the stray capacitor corresponds to the zero-sequence current of the motor. Therefore, the leakage current depends on the zero-sequence impedance, i.e., the leakage inductance and the winding resistance. On the other hand, the zero-sequence impedance has no influence on the leakage current in the case of Fig. 5(b), because the high-frequency leakage current does not flow in the motor windings. The following experiment has been performed to investigate which motor model is adequate.

Fig. 6 shows a circuit diagram to measure the cable inductance between the voltage-source PWM inverter and the induction motor. The three-phase lines are shorted on both the inverter and motor sides, and the grounding conductor is moreover shorted on the motor side. An LCR meter (HP4263A) is connected to the shorted three-phase lines and

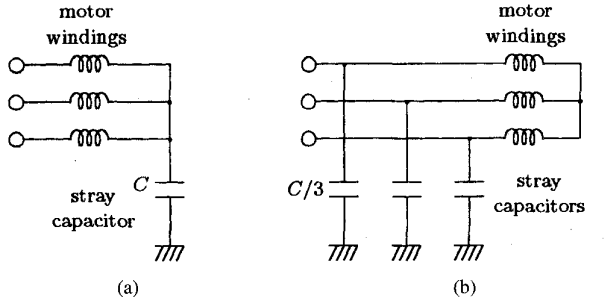

Fig. 5. Motor models.

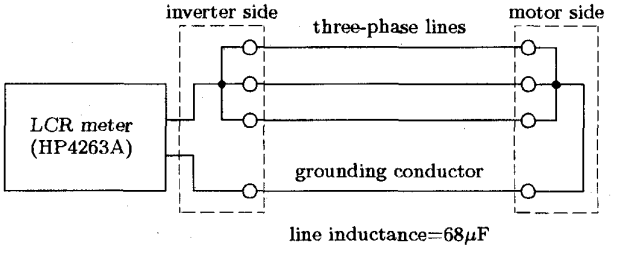

Fig. 6. Measurement of line inductance.

the grounding conductor on the inverter side. As a result, the line inductance has been measured as 68 μH. This value approximates to the inductance which has been estimated from the experimental waveform, as shown in the equivalent circuit of Fig. 4. Therefore, it can be understood that the inductance of the equivalent circuit means the line inductance between the inverter and the motor, and that the zero-sequence motor impedance has no influence on the leakage current. For this reason, Fig. 5(b) is a motor model suitable for analysis of the leakage current rather than Fig. 5(a). The proposed motor model is applicable to the analysis of both normal-mode and common-mode currents.

Generally, an equivalent circuit for a motor winding taking stray capacitors into consideration is expressed by a distributive circuit as shown in Fig. 7 [6], [7]. The equivalent circuit indicates that the high-frequency current such as the leakage current is not a conduction current flowing in the winding, but a displacement current caused by the stray capacitors. Moreover, since stator windings of a motor are embedded into slots of a stator core, there is relatively large stray capacitance between a stator winding and the motor frame rather than between two stator windings. The motor model for the high-frequency leakage current, therefore, can be simplified as a lumped circuit model shown in Fig. 5(b). On the other hand, Fig. 5(a) is a motor model suitable for analysis of the energy oscillation between the winding inductance and stray capacitors. The oscillation causes a potential variation of the neutral point [8].

In addition, measurement of the impedance between the shorted stator windings and the motor frame has been performed. As a result, the capacitance and the series resistance almost coincide with their values calculated from the experimental waveform. The measurement mentioned above leads to the following conclusions.

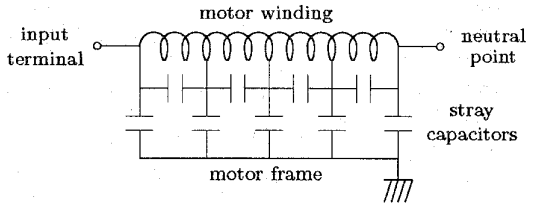

Fig. 7. Equivalent circuit for a motor winding taking stray capacitors into consideration.

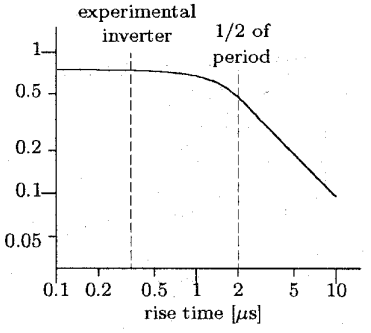

Fig. 8. Relationship between rise time and peak value.

- The equivalent circuit for the leakage current forms an LCR series resonant circuit.
- In the equivalent circuit, C is the stray capacitance between the stator windings and the motor frame.
- Almost all resistive components are in the motor rather than in the cables.
- The zero-sequence motor impedance has no influence on the leakage current.

The high-frequency leakage current is affected by the rise time of the inverter common-mode voltage. Fig. 8 shows a relationship between the rise time of voltage and the peak value, which is obtained by simulation based on the equivalent circuit shown in Fig. 4. If the rise time of the common-mode voltage is longer than 1/2 of the oscillation period, the leakage current decreases considerably. Limiting the dv/dt on the inverter output terminals is expected to have a desirable effect on conducted and radiated EMI as well as machine insulation life [8]–[10].

III. Effect of Common-Mode Choke on Leakage Currents

A. Theoretical Analysis

A common-mode choke is connected between the inverter and the motor in order to suppress the leakage current. The insertion of the common-mode choke means an increase of inductance L in the equivalent circuit. Furthermore, resistance R also increases because of the additional loss in the common-mode choke. It is assumed that inductance L and resistance R including the common-mode choke are n times and m times as large as those excluding it, respectively. In this case, the natural frequency ω_n', the damping factor ζ', and the characteristic impedance Z_0' are

$$\omega_n' = \frac{1}{\sqrt{nLC}} = \frac{1}{\sqrt{n}}\omega_n \tag{6}$$

$$\zeta' = \frac{mR}{2}\sqrt{\frac{C}{nL}} = \frac{m}{\sqrt{n}}\zeta \tag{7}$$

$$Z_0' = \sqrt{\frac{nL}{C}} = \sqrt{n}\,Z_0. \tag{8}$$

Therefore, the leakage current is given by

$$i'(t) = \frac{E}{\sqrt{n-(m\zeta)^2}\,Z_0}\cdot e^{-(m\zeta\omega_n t/n)} \cdot \sin\sqrt{n-(m\zeta)^2}\,\frac{\omega_n}{n}t. \tag{9}$$

If the damping factor is small enough, i.e., $n \gg (m\zeta)^2$, the leakage current is approximated by

$$i'(t) \simeq \frac{E}{\sqrt{n}Z_0}\cdot e^{-(m\zeta\omega_n t/n)}\sin\frac{\omega_n}{\sqrt{n}}t. \tag{10}$$

It indicates that the amplitude, the decay time, and the resonant frequency are equal to $1/\sqrt{n}$, n/m, and $1/\sqrt{n}$ times due to the addition of the common-mode choke, respectively. Table II summarizes the effect of the common-mode choke on the leakage current. Since the amplitude and the decay time are equal to $1/\sqrt{n}$ and n/m times, magnification of the rms value is calculated by

$$\sqrt{\left(\frac{1}{\sqrt{n}}\right)^2 \times \frac{n}{m}} = \frac{1}{\sqrt{m}}. \tag{11}$$

Similarly, magnification of the mean value is given by

$$\frac{1}{\sqrt{n}} \times \frac{n}{m} = \frac{\sqrt{n}}{m}. \tag{12}$$

TABLE II
Effect of Common-Mode Choke

inductance	L	n
resistance	R	m
natural frequency	ω_n	$1/\sqrt{n}$
damping factor	ζ	$m/\sqrt{n}$
characteristic impedance	Z_0	$\sqrt{n}$
decay time	$1/\zeta\omega_n$	n/m
peak value		$1/\sqrt{n}$
rms value		$1/\sqrt{m}$
mean value		$\sqrt{n}/m$

Note: The right column shows the ratio of a parameter with a common-mode choke to the corresponding one without it, respectively.

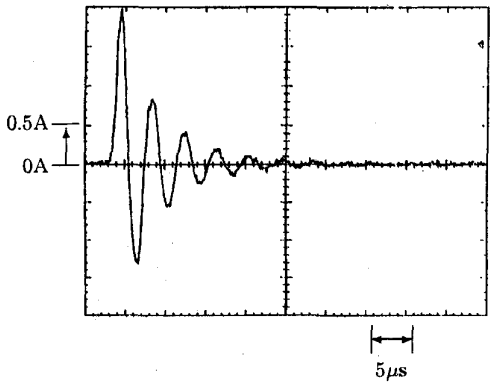

Fig. 9. Leakage current when no common-mode choke is connected.

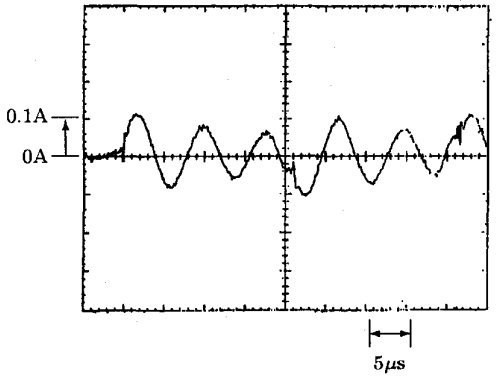

Fig. 10. Leakage current when the common-mode choke is connected.

TABLE III
PEAK AND RMS VALUES OF LEAKAGE CURRENT

common-mode choke	peak value [mA]	rms value [mA]
not used	1900	181.0
connected	108	56.6

If a common-mode choke has no loss, i.e., $m = 1$, no change occurs in the rms value, but the mean value increases, while the peak value decreases.

B. Experimental Investigation

Figs. 9 and 10 show waveforms of the leakage current, when a step-wise common-mode voltage of 280 V occurs at the output terminals of the PWM inverter. The experimental results are summarized in Table III. It is shown that a common-mode choke connected between the inverter and the motor reduces the peak value of the leakage current from 1900 mA to 181 mA. Fig. 11 represents the equivalent circuit in the case of connecting the common-mode choke. Here, the common-mode choke makes the inductance L and the resistance R increase by 380 times and 9.2 times as large as those excluding it, respectively. The peak value and the rms value in the case of connecting the common-mode choke approximate to the theoretical values, i.e., 1900 mA/$\sqrt{380}$ = 97.5 mA and 181 mA/$\sqrt{9.2}$ = 59.6 mA, respectively.

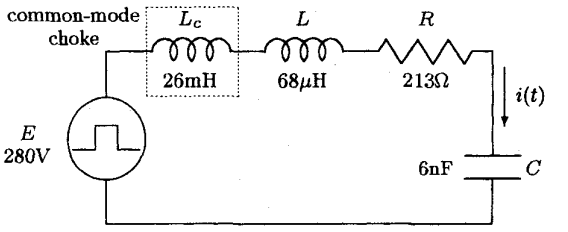

Fig. 11. Equivalent circuit for leakage current in case of connecting common-mode choke.

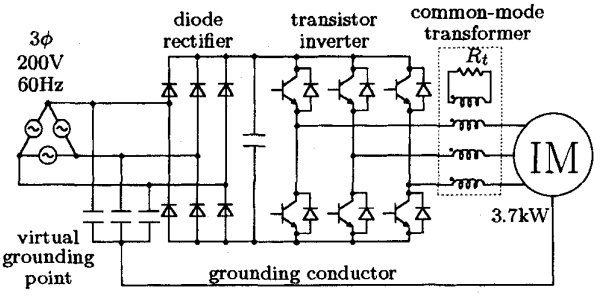

Fig. 12. Configuration of experimental system connecting common-mode transformer proposed in this paper.

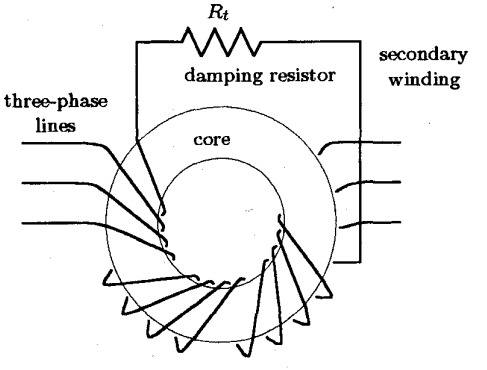

Fig. 13. Common-mode transformer proposed in this paper.

IV. EFFECT OF COMMON-MODE TRANSFORMER

Fig. 12 shows an experimental system connecting a common-mode transformer between the inverter and the motor. The common-mode transformer proposed in this paper is the same as the common-mode choke except for connecting an additional tightly coupled secondary winding, the terminals of which are shorted by a resistor R_t, as shown in Fig. 13. The common-mode current flowing in three-phase lines produces a flux in the core, but no flux is caused by the normal-mode or differential-mode current. Therefore, the common-mode transformer acts as the damping resistor only for the common-mode current, i.e., the leakage current. On the other hand, since the secondary current prevents the flux in the core from changing, the short-circuit of the secondary winding by the damping resistor makes the core compact.

A. Root Locus and Time Response of Leakage Current

Fig. 14 shows the equivalent circuit for the leakage current. The common-mode transformer is represented by a T-type

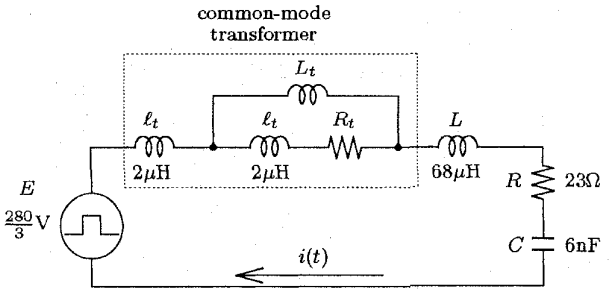

Fig. 14. Equivalent circuit for leakage current in case of connecting common-mode transformer.

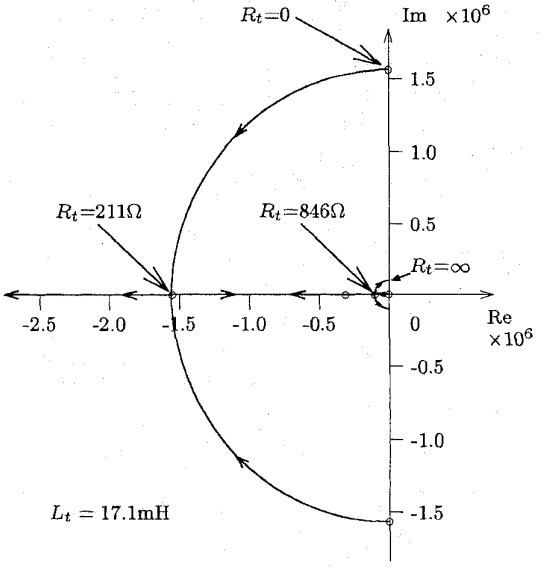

Fig. 15. Root locus.

equivalent circuit. L_t and ℓ_t mean exciting inductance and leakage inductance of the common-mode transformer, respectively. Equation 13 shows the Laplace transform of the leakage current after a step-wise common-mode voltage of E is applied to the inverter output terminals

$$I(s) = \frac{C(sL_t + R_t)E}{s^3 L_t LC + s^2(L_t + L)CR_t + sL_t + R_t}. \quad (13)$$

Here, it is assumed that ℓ_t and R are negligible in (13), because these are much smaller than L_t and R_t, respectively. Fig. 15 shows a root locus of the leakage current as a parameter of R_t.

If R_t = 0–211 Ω. there are one real root and two conjugate complex roots. The conjugate complex roots determine the waveform of the leakage current, because the real root near the origin is canceled by the zero of $I(s)$. Therefore, the leakage current becomes an oscillatory waveform. Fig. 16 shows the leakage current waveform in the case of $R_t = 0$. It is the same waveform as Fig. 3, because the common-mode transformer has no impedance for the leakage current.

If R_t = 211–846 Ω, three real roots exist. The second nearest real root to the origin mainly decides the waveform, because the nearest real root is canceled by the zero.

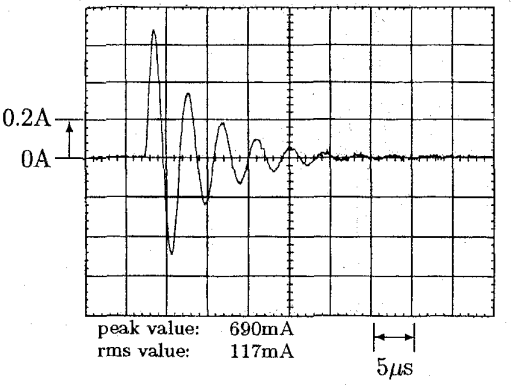

Fig. 16. Leakage current waveform (L_t = 17 mH, R_t = 0 Ω).

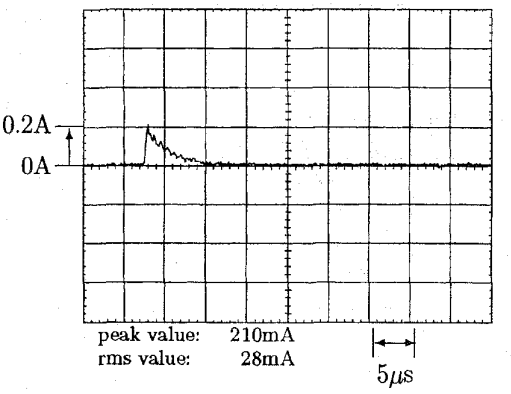

Fig. 17. Leakage current waveform (L_t = 17 mH, R_t = 510 Ω).

Consequently, the leakage current has an aperiodic decayed waveform like a current in an RC series circuit to which a step-wise voltage is applied. Fig. 17 shows the leakage current waveform in case of R_t = 510 Ω. The peak and rms values of the leakage current are reduced to 1/3 and 1/4, respectively.

If R_t = 846–∞ Ω, $I(s)$ has one real root and two conjugate complex roots again. Since the real root exists far away from the origin, the conjugate complex roots determine the waveform. However, the oscillation frequency is much lower than that in the former case, because L_t is much larger than L. Fig. 18 shows the leakage current in the case of R_t = 20 kΩ. Although the peak value is reduced to 1/9, the period and decay time of the oscillation are much longer than those in the case of Fig. 16. As a result, the rms value becomes larger than that of Fig. 17.

The analysis mentioned above results in the conclusion that the value of R_t should be selected so that $I(s)$ has three real roots, in order to reduce both peak and rms values of the leakage current.

B. Breakaway Points

In the following, resistance R_t is chosen so that the roots come onto a breakaway point. The characteristic equation corresponding to the denominator of (13) is shown by a 3rd-order equation:

$$s^3 L_t LC + s^2(L_t + L)CR_t + sL_t + R_t = 0. \quad (14)$$

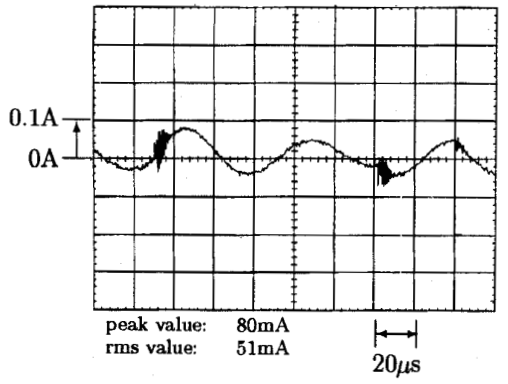

Fig. 18. Leakage current waveform (L_t = 17 mH, R_t = 20 kΩ).

From the discriminant D in Cardan's formulas [11], the following equation should be satisfied:

$$-D = \frac{4}{9^3}\left[\frac{3}{CL} - \left\{\frac{(L_t+L)R_t}{L_tL}\right\}^2\right]^3 + \frac{1}{27^2}\left[2\left\{\frac{(L_t+L)R_t}{L_tL}\right\}^3 - \frac{9(L_t+L)R_t}{CL_tL^2} + \frac{27R_t}{CL_tL}\right]^2. \quad (15)$$

Assuming that $L_t \gg L$, the above equation is simplified:

$$\frac{4}{L_tL}R_t^4 - \frac{1}{CL}R_t^2 + \frac{4}{C^4} = 0. \quad (16)$$

The solution of the above equation is given by

$$\begin{aligned} R_t^2 &= \frac{L_tL}{8}\left\{\frac{1}{CL} \pm \sqrt{\frac{1}{C^2L^2} - \frac{64}{L_tLC^2}}\right\} \\ &= \frac{L_t}{8C}\left\{1 \pm \sqrt{1 - 64\frac{L}{L_t}}\right\} \\ &\approx \frac{L_t}{8C}\left\{1 \pm \left(1 - 32\frac{L}{L_t}\right)\right\} \\ &\approx \frac{1}{4}\cdot\frac{L_t}{C} \quad \text{or} \quad 4\cdot\frac{L}{C}. \end{aligned}$$

Therefore, R_t at the breakaway points are solved as follows:

$$R_t = \frac{1}{2}Z_{0\infty} \quad \text{or} \quad 2Z_{00}. \quad (17)$$

where

$$Z_{0\infty} = \sqrt{\frac{L_t}{C}} \quad (18)$$

$$Z_{00} = \sqrt{\frac{L}{C}}. \quad (19)$$

$Z_{0\infty}$ and Z_{00} mean the characteristic impedances in the cases of $R_t = \infty$ and $R_t = 0$, respectively. If (17) is satisfied, the roots of (13) are on the corresponding breakaway point. If R_t satisfies the following condition, $I(s)$ has three real roots, so that both peak and rms values of the leakage current can be reduced

$$2Z_{00} \leq R_t \leq \tfrac{1}{2}Z_{0\infty}. \quad (20)$$

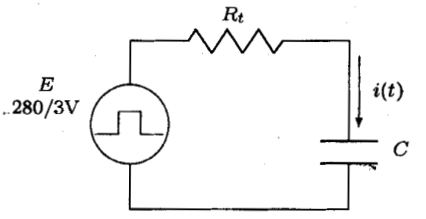

Fig. 19. Equivalent circuit approximated to RC series circuit.

V. Design of Common-Mode Transformer

A design procedure of common-mode transformers is discussed, assuming that stray capacitances are known. The equivalent circuit, having three real roots, can be approximated to an RC series circuit shown in Fig. 19, because the leakage current flows mainly through R_t rather than through L_t. In this case, the leakage current is approximated as follows:

$$i(t) = \frac{E}{R_t}e^{-t/CR_t} \quad (21)$$

where E means 1/3 of the dc link voltage. Assuming that the time constant is much smaller than the switching period, the rms value of the leakage current is given by

$$\begin{aligned} I_{rms} &= \sqrt{\frac{6}{T}\int_0^\infty i(t)^2dt} \\ &= E\sqrt{\frac{3C}{R_tT}}. \end{aligned} \quad (22)$$

Note that the switching is 6 times the PWM frequency while operating in the linear range.

The rms value of the leakage current should be specified in advance of the design. For example, sensitivity of a residual current-operated circuit breaker (3ϕ3 W, 200 V, 30 A) is rated as 30 mA. If I_{rms} is specified, the required resistance R_t can be calculated backward:

$$R_t = \frac{3CE^2f_{sw}}{I_{rms}^2}. \quad (23)$$

On the other hand, the power loss dissipated in resistor R_t is easily given by the equivalent RC circuit:

$$P_{Rt} = 6\cdot\tfrac{1}{2}CE^2f_{sw}. \quad (24)$$

As shown in (20), R_t must satisfy the condition of $R_t \leq \frac{1}{2}\sqrt{L_t/C} = \frac{1}{2}Z_{0\infty}$, so that $I(s)$ has three real roots and both peak and rms values can be reduced. To minimize L_t, which is related to the size of the common-mode transformer, R_t should be equal to half of $Z_{0\infty}$. Therefore, the exciting inductance

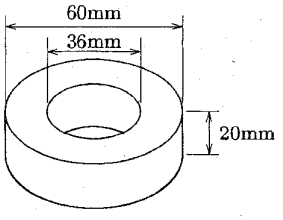

Fig. 20. Shape of toroidal ferrite core.

TABLE IV
SPECIFICATION OF TOROIDAL FERRITE CORE

TYPE	H1D T60×20×36 (TDK)	
A_e	235	mm^2
ℓ_e	144	mm
AL	13.2±25%	$\mu H/N^2$
Wt	172	g
B_s	430(at 25°C)	mT
	260(at 100°C)	mT

L_t can be determined as follows:

$$L_t = 4R_t^2 C = \frac{36C^3E^4f_{sw}^2}{I_{rms}^4}. \quad (25)$$

Furthermore, the following equation gives the maximum linkage flux $\Phi_{\max}$ in the secondary winding, because the same voltage as that across the resistor is applied to the exciting inductance:

$$\Phi_{\max} = 3CR_tE = 9\frac{C^2E^3f_{sw}}{I_{rms}^2}. \quad (26)$$

As mentioned above, L_t and $\Phi_{\max}$ are important parameters to design the core of the common-mode transformer.

VI. PROTOTYPE COMMON-MODE TRANSFORMER

A prototype common-mode transformer is constructed and tested in order to verify the effect on the leakage current. Fig. 20 shows the shape of a ferrite core used in the prototype, and Table IV shows the specification of the ferrite core.

If the rms value of the leakage current, I_{rms} is specified as 27 mA, R_t, P_{Rt}, L_t, and $\Phi_{\max}$ calculated by (23)–(26) are 516 Ω, 0.38 W, 6.4 mH, and 866 μWb, respectively. The number of turns N is given by the AL-value of the ferrite core:

$$N = \sqrt{\frac{L_t}{AL}} = 22. \quad (27)$$

Therefore, the effective sectional area A_e gives the maximum flux density

$$B_{\max} = \frac{\frac{\Phi_{\max}}{N}}{A_e} = 188\,\text{mT} \quad (28)$$

and it is much smaller than saturation flux density B_s of the core material (H1D). This result indicates that an optimal design of the core shape would make the common-mode transformer more compact. Fig. 21 shows the photograph of the common-mode transformer. A damping resistor of 510 Ω, 0.5 W is connected to the terminals of the secondary winding, because the power loss dissipating in the damping resistor is calculated as 0.38 W.

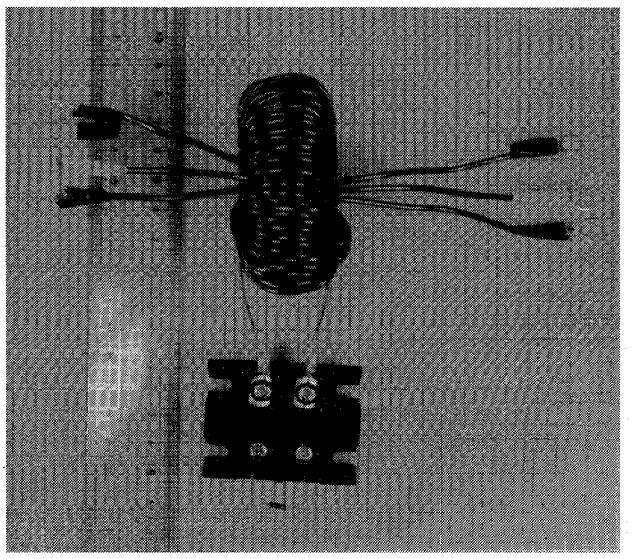

Fig. 21. Photograph of prototype common-mode transformer.

Fig. 22 shows the characteristics of the rms leakage current I_{rms}, the maximum linkage flux $\Phi_{\max}$, and the power loss P_{Rt} with respect to R_t at $L_t = 6.4$ mH, respectively. Simulation for the equivalent circuit shown in Fig. 14 is performed, using the PSpice circuit simulator. The simulation results are shown as the solid lines, while the experimental results are plotted. It shows the validity of the modeling for the leakage current as well as the effectiveness of the common-mode transformer. The measured values agree well with the simulated ones, and I_{rms} is reduced to 25% at the designed point of $R_t = 510\,\Omega$. $\Phi_{\max}$ at $R_t = 510\,\Omega$ is smaller than the designed value calculated by (26), because R_t attenuates the exciting current. Connecting the damping resistor $R_t = 1$ kΩ corresponds to the case that the actual stray capacitance is 2 times as large as the designed value. Comparing this point with the designed point, $\Phi_{\max}$ increases to 1.5 times though I_{rms} decreases slightly. It means that the common-mode transformer can reduce the high-frequency leakage current even if the normal variance in the values of the stray capacitance exists, although some margin in the flux density is required to prevent the core from magnetic saturation. Finally, the leakage current waveform in case of connecting the prototype common-mode transformer is shown in Fig. 23, which is the same waveform as Fig. 17.

A common-mode transformer, the secondary winding of which is open, is equivalent to a conventional common-mode choke having the same inductance as the exciting inductance of the common-mode transformer. $\Phi_{\max}$ at $R_t = 500\,\Omega$ is 1/3 of that at $R_t = \infty$. This makes a great contribution to reducing the core size of the common-mode transformer compared with that of the conventional common-mode choke.

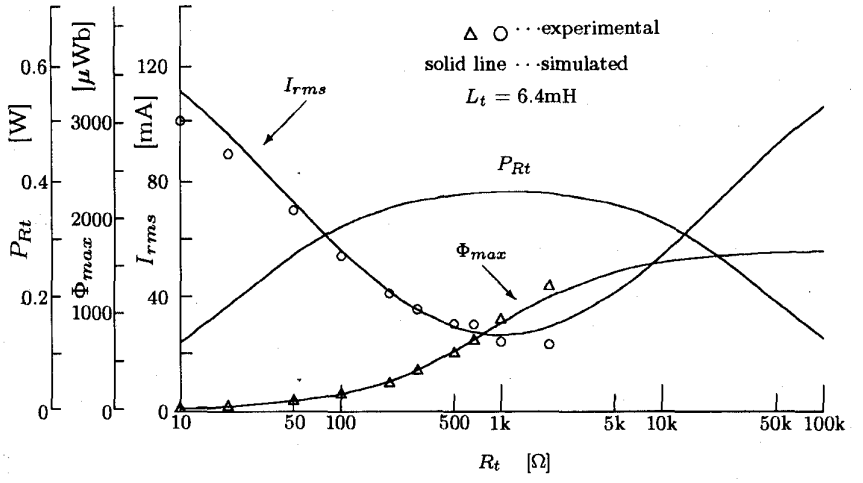

Fig. 22. Effect of common-mode transformer.

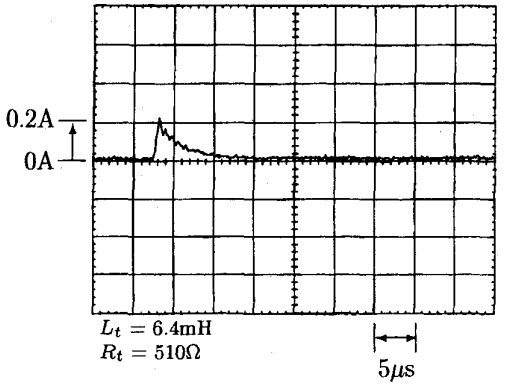

Fig. 23. Leakage current in case of connecting prototype common-mode transformer.

VII. Conclusions

In this paper, the high-frequency leakage current in PWM inverter-fed ac motor drives has been discussed in detail. The analyses and the experiments described in this paper lead to the following consequences.

- The equivalent circuit for the leakage current is represented as an LCR series resonant circuit.
- The zero-sequence impedance of ac motors has no influence on the leakage current.
- Conventional common-mode chokes are not effective to reduce the rms and average values of the leakage current, but effective to reduce the peak value.

Furthermore, a common-mode transformer has been proposed, which is able to reduce both the peak and rms values of the leakage current. The design procedure of the common-mode transformer has also been presented. A prototype common-mode transformer, dissipating a negligible amount of loss, has been constructed and tested in a vector controlled induction motor of 3.7 kW. It has been confirmed that the peak and rms values of the leakage current are reduced to 1/3 and 1/4, respectively, while the core size of the common-mode transformer is also reduced to 1/3 of that of a conventional common-mode choke. The authors believe that the common-mode transformer proposed in this paper is an effective alternative to the conventional common-mode choke.

References

[1] J. L. Norman Violette, D. R. J. White, and M. F. Violette, *Electromagnetic Compatibility Handbook.* New York: Van Nostrand Reinhold, 1987.
[2] C. R. Paul and K. B. Hardin, "Diagnosis and reduction of conducted noise emissions," *IEEE Trans. Electromag. Compat.*, vol. 30, no. 4, Nov. 1988.
[3] N. Mohan, T. M. Undeland, and W. P. Robbins, *Power Electronics: Converters, Applications and Design.* New York: Wiley, 1989.
[4] M. A. Jabbar and M. Azizur Rahman, "Radio frequency interference of electric motor and associated controls," *IEEE Trans. Ind. Applicat.*, vol. 27, pp. 27–31. Jan./Feb. 1991.
[5] Y. Murai, T. Kubota, and Y. Kawase, "Leakage current reduction for a high-frequency carrier inverter feeding an induction motor," *IEEE Trans. Ind. Applicat.*, vol. 28, pp. 858–863, July/Aug. 1992.
[6] E. Zhong, S. Chen, and T. A. Lipo, "Improvement in EMI performance of inverter-fed motor drives," in *APEC 94 Conf. Rec.*, vol. 2, pp. 608–614, 1994.
[7] B. Heller and A. Veverka, *Surge Phenomena in Electrical Machine.* Iliffe Books Ltd., 1968.
[8] R. E. Pretorius and A. J. Eriksson, "A basic guide to rc surge suppression on motors and transformers," *Trans. SA Inst. Elec. Eng.*, pp. 201–209, Aug. 1980.
[9] G. Venkataramanan and D. M. Divan, "Pulse width modulation with resonant dc link converters," *IEEE Trans. Ind. Applicat.*, vol. 29, pp. 113–120, Jan./Feb. 1993.
[10] B. K. Bose, "Power electronics and motion control—Technology status and recent trends," *IEEE Trans. Ind. Applicat.*, vol. 29, pp. 902–909, Sep./Oct. 1993.
[11] I. N. Herstein, *Topics in Algebra,* 2nd ed. New York: Wiley, 1975.

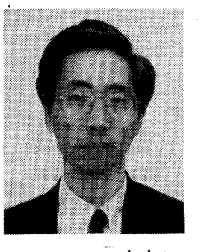

Satoshi Ogasawara (A'87–M'93) was born in Kagawa prefecture, Japan, on August 27, 1958. He received the B.S., M.S., and Dr.Eng. degrees in electrical engineering from Nagaoka University of Technology, Niigata, Japan, in 1981, 1983, and 1990, respectively.

From 1983 to 1992, he was a Research Associate at the Nagaoka University of Technology. Since 1992, he has been with the Department of Electrical Engineering, Okayama University, Okayama, Japan, and he is currently an Associate Professor. His present research interests are in ac motor drives systems and static power converters.

Dr. Ogasawara is a member of the Institute of Electrical Engineers of Japan.

Hirofumi Akagi (M'87–SM'94–F'96) was born in Okayama, Japan, on August 19, 1951. He received the B.S. degree from Nagoya Institute of Technology in 1974 and the M.S. and Ph.D. degrees from Tokyo Institute of Technology in 1976 and 1979, respectively, all in electrical engineering. In 1979, he joined Nagaoka University of Technology as an Assistant and then Associate Professor in the Department of Electrical Engineering. In 1987, he was a visiting scientist at Massachusetts Institute of Technology for ten months. Since 1991, he has been a Professor in the Department of Electrical Engineering at Okayama University. His research interests include power electronic circuits and systems, and their industrial and utility applications.

Dr. Akagi is a corecipient of the first-prize paper award in the IEEE Transactions on Industry Applications for 1991 and four IEEE/IAS committee prize paper awards.